SCIENCE CHINA
Chemistry

• ARTICLES •

April 2015 Vol.58 No.4: 658–665
doi: 10.1007/s11426-014-5212-x

Dicyanovinyl-unit-induced absorption enhancement of iridium(III) complexes in long-wavelength range and potential application in dye-sensitized solar cells

Dongdong Wang[1*], Hua Dong[2], Xiaoyu Zhang[3], Yong Wu[1], Shaohua Shen[4], Bo Jiao[2], Zhaoxin Wu[2], Min Gao[1] & Geng Wang[1]

[1]*Department of Applied Chemistry, School of Science, Xi'an Jiaotong University, Xi'An 710049, China*
[2]*Key Laboratory for Physical Electronics and Devices of the Ministry of Education, School of Electronic and information Engineering, Xi'An Jiaotong University, Xi'An 710049, China*
[3]*Key Laboratory for Advanced Materials, Institute of Fine Chemicals and Department of Chemistry, East China University of Science and Technology, Shanghai 200237, China*
[4]*International Research Center for Renewable Energy, State Key Laboratory of Multiphase Flow in Power Engineering, Xi'an Jiaotong University, Xi'An 710049, China*

Received May 8, 2014; accepted May 27, 2014; published online November 6, 2014

Iridium complexes with dicyanovinyl-grafted phenylpyridine/1-phenylisoquinoline as ligands are synthesized and their photophysical, electrochemical, and sensitization properties in DSSCs are investigated. The iridium complexes present significantly enhanced absorption from 400 to 525 nm. The 1-phenylisoquinoline-based iridium complex show bathochromic-shift emission in DMSO solution compared with their phenylpyridine-based counterpart, while their absorption response and photoluminescence peak in solid show little difference despite extension of the conjugated system. Using DSSCs, the conversion efficiency of 0.62% and open-circuit current of 1.4 mA/cm^2 is achieved. The poor performance is attributed to the excited-state properties of iridium complexes according to the TD-DFT calculation.

dicyanovinyl group, iridium complexes, absorption response, dye-sensitized solar cell

1 Introduction

Cyclometalated iridium(III) complexes have recently attracted considerable attention due to their applications in electroluminescence [1], photocatalysis [2], phosphorescent molecular probes [3], etc. Yet, the true strength of the iridium complexes is found as phosphorescent materials in organic light-emitting diodes (OLEDs), which are crucial for the highly efficient device performances because of high photoluminescence quantum yields, relatively short excited-state lifetime, and excellent color tunability. However, the development of Ir(III) complexes for applications in visible-light harvesting fields is a nascent stage, mainly because the excitation wavelengths of typical cyclometalated Ir(III) complex are located in the UV or blue region and their molar extinction coefficient is very low in the visible-light region [4]. As a result the key parameter, overall conversion efficiency of solar-cell-based on Iridium complexes, is far from competing with that of ruthenium complex [5]. However, despite the poor characteristics of the device, compared to the ruthenium complexes that are usually used, iridium complexes have been demonstrated to have several advantages such as higher stability, less-accessible MC (metal-centered) state, and the potential for dual sensitization through LLCT (ligand-to-ligand charge transfer) and MLCT (metal-to-ligand charge transfer). Although the

*Corresponding author (email: ddwang@mail.xjtu.edu.cn)

ruthenium dyes show the most efficient devices, but the lowest excited state of the ruthenium complexes has MLCT character, which is very sensitive to spatial separation (r) of an electrode surface. Therefore, a general strategy for reduction of the recombination of charges [5,6] could be obtained by further improvement of device performance. In this respect, development of of an iridium complex for DSSC (dye-sensitized solar cells) is highly desirable and improvement of their absorption properties is certainly a key factor.

To date, only a few iridium complexes for DSSC application have been reported. For most of them, the absorption response them is less than 400 nm [5]. Recently, several iridium complexes have been documented to show enhanced absorption capacity, from 400 to 500 nm, by modifying phenylpyridine ligand with oligothiophene pendants [7] or oligofluorene segment [8], or using 7-diethyaminocoumarine auxiliary ligand [9], etc. [10]. However, these iridium complexes cannot be applied to DSSC. Recently, we found that introducing dicyanovinyl substituent into phenyl *meta*-position of ppy (phenylpyridine) in iridium (III) bis(phenylpyridinato)picolinate can induce a significant enhancement of absorption capacity in the visible-light range, from 400 to 500 nm. In addition, its oxidation potential is sufficiently positive to oxidize the I_3^-/I^- redox couple, which makes it a good candidate for use in DSSCs. In the molecule (iridium(III) bis(5-dicyanovinylphenylpyridinato) picolinate), herein called control complex, the dicyanovinyl group behaves as an electron-withdrawing moiety with extended π-conjutate length and induces a change in the electron density of the ligands, thereby tuning the orbital energetics and directly affecting the electronic transition of the resulting iridium complexes, which feature intense absorption and a broader spectral response in the visible-light range [11].

Encouraged by this finding, we proceeded to synthesize the counterparts of these iridium complexes with a classic acid-anchoring group (Scheme 1) consisting of Ir(III)bis(5-dicyanovinylphenylpyridinato)-4-carboxylpicolinate (**4a**) and Ir(III)bis(5-dicyanovinylphenylpyridinato)-4,4′-dicarbo-

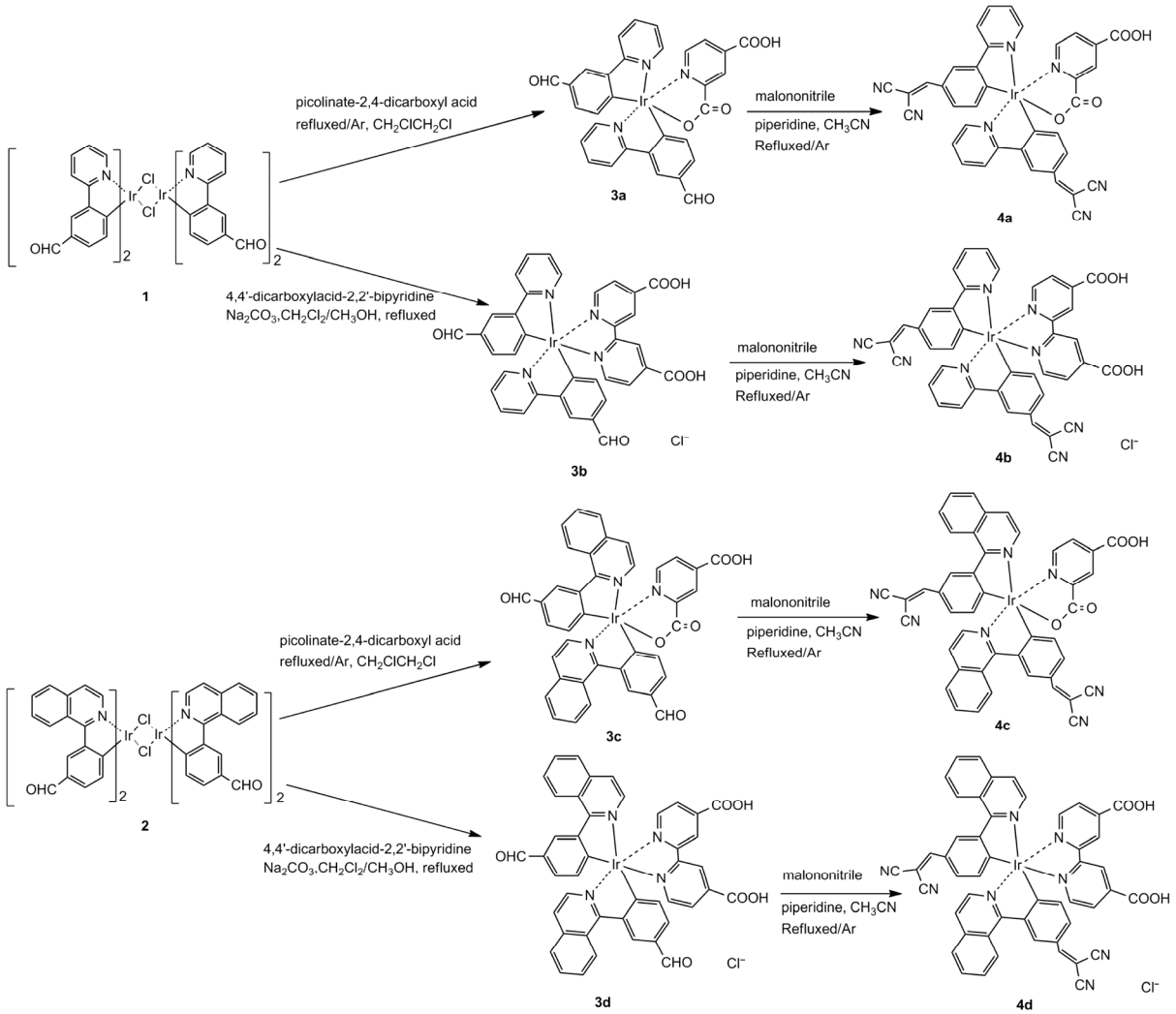

Scheme 1 The synthesis route of iridium complexes **4a**–**4d**.

xylacid-2,2′-bipyridine (**4b**), as well as 1-phenylisoquinoline-based iridium complexes instead of pyridine ring (**4c** and **4d**). Their photophysical and electrochemical properties, photovoltaic performances, and sensitization behaviors in solar cells were investigated.

2 Experimental

Scheme 1 shows the synthetic route of the iridium complexes. Complexes **4a** and **4c** were prepared according to our previously published procedure [11]. The chloro-bridged iridium(III) dimmer first reacted with 2,2′-bipyridine-4,4′-dicarboxylic acid to afford complexes **3b** and **3d** in the presence of Na_2CO_3, then reacted with malononitrile in acetonitrile solution to produce the final product **4b** and **4d**. Detailed experimental procedures are provided in Supporting Information online.

The steady-state absorption in solution and on TiO_2-dyes-adsorbed films was measured using Hitachi (U-3310, Japan) spectrophotometers and a Varian Cary 500 spectrophotometer (USA), respectively. Emission spectra were recorded with Edinburgh FS920 fluorometers (UK). Cyclic voltammetry (CV) was measured on a Princeton Applied Research Model 273 A electrochemical workstation (USA). A three-electrode system was selected in which a glassy carbon was used as working electrode, and Pt-sheet and Pt-wire were used as counter-electrode and reference electrode, respectively. The oxidation measurement for complexes **4b** and **4d** was done in anhydrous CH_3CN solution containing 0.1 mol/L TBAPF6 as supporting electrolyte; for complexes **4a** and **4c**, CH_2Cl_2 solution was used. The reduction measurements were recorded in DMSO for all of the complexes. The potentials were measured against the Pt-wire reference electrode with ferroceninium/ferrocence (Fc/Fc^+) as internal standard. The scan rate for all the measurements was 100 mV/s.

DSSCs were fabricated in reference to the literature [12]. Glass-substrate-coated FTO sheets (Nippon Sheet Glass, Japan) of 2.2 mm thickness, 14 Ω/sq, were cleaned using an ultrasonic bath in detergent solution for 30 min, then rinsed for 30 min with deionized water, isopropanol, and EtOH, respectively. A transparent TiO_2 paste (P90 Degussa, 15 nm) was screen-printed to form a first transparent layer and dried at 125 °C for 6 min. This procedure was repeated until the appropriate thickness of 12 μm of TiO_2 was obtained for use as the working electrode. Subsequently, a 5 μm light-scattering layer containing 200 nm anatase of TiO_2 was deposited on TiO_2 electrode by screen-printing and then thermally treated in sequence under air flow at 325 °C for 5 min, 375 °C for 10 min, 450 °C for 15 min, and 500 °C for 15 min at a heating ramp rate of 5–10 °C/min. The sintered layer was treated again with 40 mmol/L titanium tetrachloride-aqueous solution (70 °C for 30 min), rinsed with water and EtOH, and heated at 450 °C for 30 min. After cooling down to 80 °C, the TiO_2 electrode was immersed into a CH_2Cl_2/ CH_3OH (4:1, *v*/*v*) solution containing iridium complex sensitizer (300 μmol/L) and cheno (2 mmol/L) for 21 h. After that, the dye-absorbed TiO_2 electrode and the Pt-nanoparticle-structured counter-electrode were assembled into a sealed sandwich-type cell using a Bynel 60 μm hot-melt ionomer film (Dupont, USA) as a spacer between them. Finally, the electrolyte solution was introduced into the cell through a hole and sealed with a hot-melt Bynel ionomer film and a glass cover. The electrolyte of all of the cells contained 0.6 mol/L 1-butyl-3-methyl imidazolium iodide (BMII), 0.03 mol/L I_2, 0.02 mol/L LiI, 0.10 mol/L guanidinium thiocyanate, and 0.5 mol/L 4-*tert*-butylpyridine in a mixture of acetonitrile and valeronitrile (85:15, *v*/*v*). The active area of each cell was typically 0.25 cm^2.

A Keithley 2400 source (USA) was used to record the current-density voltage (*J*-*V*) characteristics of the DSSCs under the illumination of AM 1.5 G simulated solar light (Newport-91160, USA) equipped with a 300W Xe lamp and an AM 1.5 G filter, in which the incident light intensity was calibrated to 100 mW/cm^2 with a standard silicon solar cell (Newport 91150V, USA). A Newport 74125 system (Newport Instruments, USA), in which the intensity of monochromatic light was measured with a Si detector (Newport-71640, USA), was used to measure the incident monochromatic photon-to-electron conversion efficiency (IPCE) for the solar cells. A Zahner IM6e Impedance Analyzer (ZAHNER-Elektrik GmbH & CoKG, Kronach, Germany) was used to obtain the electrochemical impedance spectroscopy (EIS) measurements of all the DSSCs. The applied voltage bias and the magnitude of the alternative signal were fixed at –0.40 V and 10 mV, respectively. The frequency range for all of the measurements was 0.1 Hz–100 kHz.

3 Results and discussion

3.1 Synthesis, UV and emission spectra

The UV-Vis absorption spectra of all the complexes, measured in the mixed solvents of CH_2Cl_2/CH_3OH (3:1, *v*/*v*) and bound to the transparent TiO_2 film, are presented in Figure 1. The corresponding photophysical and spectra datas are summarized in Table 1. Figure 1(a) indicates that the five iridium complexes show very similar absorption profiles. It was observed that the absorption curve of complex **4a** completely coincided with that of the control complex, which suggests that introduction of an additional acid-anchoring group into the 4-position of 2-picolinic acid in the control moiety had no effect on the overall absorption response of the resulting complex. A noteworthy blue-shift absorption response was observed in both complexes **4b** and **4d** when the picolinic acid ligand in complexes **4a** and **4c** was replaced by 2,2′-bipyridine-4,4′-dicarboxyl acid. For complexes **4c** and **4d**, it was expected that broadening of the

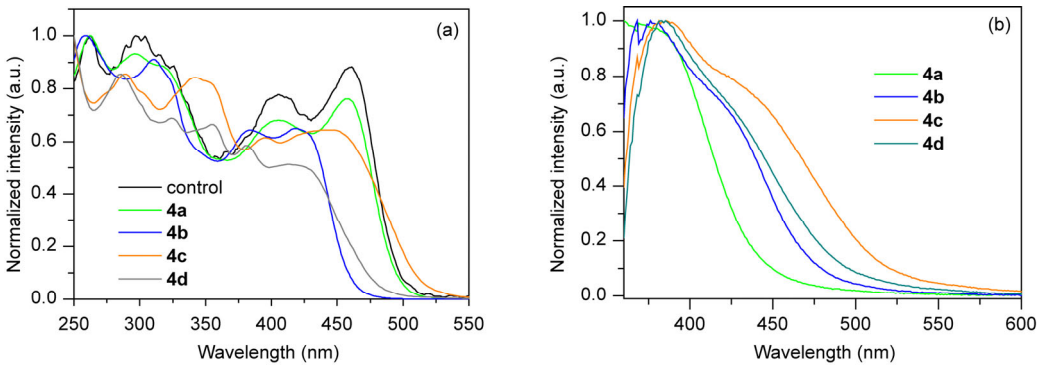

Figure 1 The absorption spectra of the iridium complexes **4a**–**4d**. (a) In solution of CH_2Cl_2/CH_3OH (3:1); (b) on TiO_2 film.

Table 1 The photophysical properties of the iridium complexes

	λ_{abs} (nm) [a]	λ_{em} (nm)	τ (ns) [d]	$E_{1/2(OX)}/E_{1/2(Re)}$ (V) [g]	HOMO [h]/LUMO [i]
Control complex	262, 299, 408, 462	516 [b]/581 [c]	252	0.93 [e]/ –	5.73/3.25
4a	262, 296, 406, 459	521 [b]/603 [c]	169	0.97 [e]/–1.01	5.77/3.27
4b	288, 342, 396, 446	527 [b]/587 [c]	113	0.62 [f]/–1.08	5.42/2.77
4c	259, 311, 383, 419	599 [b]/589 [c], 630 (sh)	306	0.95 [e]/–1.09	5.75/3.42
4d	286, 324, 356, 382, 414	602 (sh), 634 [b]/587 [c], 620 (sh)	331	0.63 [f]/–1.15	5.43/2.93

a) Measured in CH_2Cl_2/CH_3OH (3:1, *v*/*v*) at 1×10^{-6} mol/L; b) in 1×10^{-5} mol/L solution of the DMSO; c) measured in 5% iridium complexes doped PMMA film and the excited wavelength at 450 nm for **4a**–**4d**; d) lifetime measured in 5% iridium complex doped PMMA film; e) the value measured in CH_2Cl_2 and correcting relative to the value of Fe $Cp^{0/+}$; f) measured in CH_3CN vs. Fe $Cp^{0/+}$; g) the reduction process was measured in DMSO vs. Fe $Cp^{0/+}$; h) the HOMO energy level was estimated with the following formula: HOMO(eV)=$E_{1/2(OX)}$+4.80; i) LUMO=HOMO–ΔG. The absorption onset estimated from absorption spectrum in CH_3OH/CH_2Cl_2 solution.

absorption band toward lower energy could be achieved by replacing pyridine heterocycle of complexes **4a** and **4b** with an extended conjugated isoquinoline unit; however, we observed that this substitution only slightly shifted the low-energy optical absorption edge toward the longer-wavelength side. On the whole, these iridium complexes showed significantly enhanced absorption response, from 400 to about 525 nm, which suggests promising applications for photosensitizer (PS) of DSSC and other light-harvesting materials in hydrogen photogeneration, etc. When these iridium complexes were anchored onto the surface of the transparent TiO_2 film, a significant change in absorption profile, from 350 to 500 nm, was observed along with a slight blue-shift of the maximum absorption peak (Figure 1(b)). These results could be attributed to the interaction of the anchoring group with the surface of TiO_2. The absorption curves also reveal that the dyed film in complex **4c** was able to absorb more visible light than the TiO_2 film sensitized by complexes **4b** and **4d**, which in turn were better than film sensitized by complex **4a**. The reason that the TiO_2 film sensitized by complex **4a** showed such obvious blue-shift absorption spectra is unclear for the moment, unlike analogue **4c**, which included the same pyridine-2,4-dicarboxyl acid-anchoring ligand.

Figure 2 shows the photoluminescence (PL) spectra of the iridium complexes in both DMSO solution and 5%-doped PMMA (polymethymethacrylate) film, the relevant data are summarized in Table 1. Similar to the absorption spectra, complex **4a** in DMSO solution showed a green emission with peak wavelength of 521 nm, which completely coincided with that of the control complex. A slightly red-shifted (about 6 nm) and broadened emission was observed in complex **4b** when the picolinic acid auxiliary ligand was replaced with 2,2′-bipyridine-4,4′-dicarboxyl acid. We also noted that the replacement of the pyridine ring by the isoquinoline unit induced a clearly red-shifted emission and that the resulting complexes **4c** and **4d** presented red emissions with wavelengths of 599 and 634 nm, respectively. Such behavior, however, did little to adjust the absorption response to the longer wavelength. The emission spectrum of complex **4d** was characterized by an occurrence of a shoulder at about 602 nm on the high-energy side of the maximum peak, 634 nm, which revealed the nature of the triplet-excited state in complex **4d** [8]. For the PL spectra in solid film (Figure 2(b)), ppy-based iridium complexes **4a** and **4b** presented a significantly red-shifted emission compared with their emissions in solution. This result can be understood in terms of a poorly conjugated effect between the dicyanovinyl group and the benzene ring in solution, due to the free rotation of the dicyanovinyl group. By contrast, the rotation was limited in solid film, which led to a higher degree of conjugation between them as well as to a bathochromic-shift emission. Similar phenomena were observed in the control complex. By contrast, the PL spectra

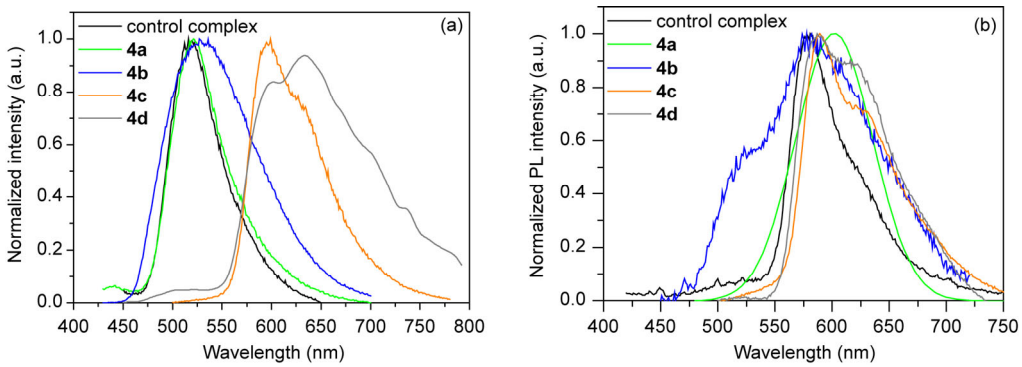

Figure 2 Normalized photoluminescence spectra of the iridium complex **4a–4b**. (a) In solution of DMSO; (b) in iridium dye-doped PMMA film.

of piq-based iridium complexes **4c** and **4d** in both solution and solid film showed no obvious differences in terms of emission maximums and spectral profiles. Based on the emission maximum in solid film, the excited-state lifetimes of all the complexes were analyzed by time-resolved excited-state decay curves. These iridium complexes have excited-state lifetimes of 113–331 ns in solid film, which are comparable to those of the Ru(II) complex that is usually used. In addition, the phenylisoquinoline-based complexes **4c** and **4d** appeared to have longer lifetimes compared with phenylpyridine-based complexes **4a** and **4b**.

3.2 Electrochemistry

To estimate the frontier molecule orbital energy, particularly HOMO energy levels based on the ionization potential for the first oxidation, cyclic voltammetry (CV) experiments were carried out in $CNCH_3$ or CH_2Cl_2 in terms of the solubility of these complexes. The CV curves are shown in Figure S1 (Supporting Information online), the electrochemical data are listed in Table 1. The oxidation potential for all the complexes occurred within a close range, from 0.62 to 0.97 V, versus the range produced by ferrocence. This oxidation process was usually assigned to the Ir(III)/Ir(IV) couple [13, 14]. Note that the oxidation potentials of all the complexes are more positive than that of I^-/I_3^- redox couple (0.4 V vs. NHE). Recent studies shown that 0.5–0.6 eV driving force is need for regeneration of dyes in I^-/I_3^- electrolyte [15]. Therefore, this driving force is sufficient for the regeneration of iridium complexes. For the reduction process, all of the complexes exhibited irreversible reduction processes, which are usually documented to primarily occur on the chelated ligands that surround the central metal. The reduction potentials for all the complexes were in the range from −1.08 to −1.15V relative to ferrocence, more negative than that of the conduction-band edge of TiO_2 (–0.5 V vs. NHE at pH 7). These results indicate that the electron-injection for TiO_2 is also sufficient. In addition, an irreversible reduction process makes the direct determination of the LUMOs energy levels from electrochemical measurements unreliable. Alternatively, the optical LUMOs energy was calculated (Table 1).

3.3 DFT calculations

To gain more insight into the enhanced absorption property in longer wavelengths of all the iridium complexes, molecule orbital (MO) calculations were performed. The HOMOs and LUMOs orbitals of electronic ground states for the iridium complexes are depicted in Figure 3, other orbitals are presented in Figures S2–S5 (Supporting Information online). The orbital compositions of the HOMO and LUMO differ little. The HOMO orbital has an important Ir dπ contribution for compexes **4a–4d**; the remainning contributions come from π orbitals located on C^N ligands. The LUMO orbital for these four complexes primarily resided on the ancillary N^N or pic ligands, mixed with very minor contributions from the Ir d orbital or C^N ligands. It is interesting to note that the LUMO of complex **4a** is more delocalized over the two C^N ligands, aside from the main contribution of the pic ligand. For other LUMO orbitals, the C^N ligand appears to have considerable contribution aside from that of the ancillary N^N ligand. On the basis of the DFT calculations, the electron transition in the low-energy region for complexes **4a–4d** is mainly attributed to MLCT and/or LLCT transition.

A time-dependent density functional theory (TD-DFT) calculation of the vertical singlet-state transition in CH_2Cl_2 was performed to obtain more information about the absorption processes and to assist with interpretation of the excited states. The calculated absorption spectra are shown in Figure S6 (Supporting Information online) and the transitions with significant oscillator strength are summarized in Table S1 (Supporting Information online). As in Figure S6, the computed singlet transitions are generally in good agreement with the experimental results in terms of excitation intensity and energy. For iridium complexes **4a**, **4b**, **4c**, and **4d**, the computed HOMO-LUMO-type singlet transi-

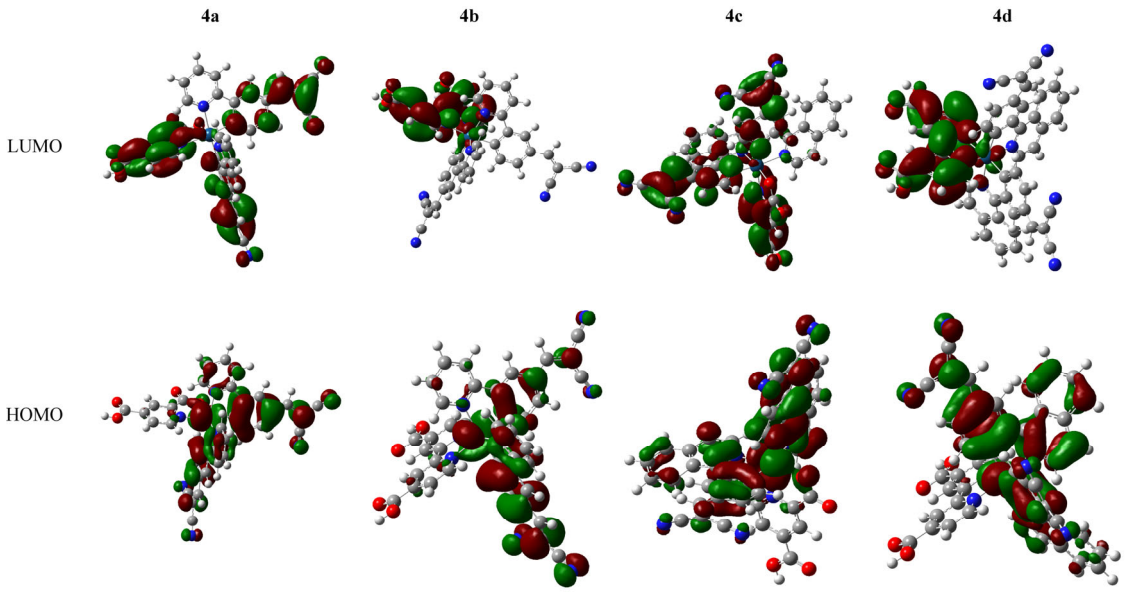

Figure 3 The calculated contours of the HOMOs and LUMOs orbitals of the iridium complexes **4a**–**4d**.

tions at 428.5 (S_1 with oscillator strength f=0.1156), 490.1 (S_4, f=0.0205), 467.2 (S_1, f=0.0801), and 498.4 nm (S_1, f= 0.0093) are all attributed to the beneficial charge transfer from Ir dπ or C^N ligand π orbitals to the anchoring ligand. The computed band with higher energy at 412.7 nm for complex **4a** is attributed to a transition to the third-singlet excited state (S_3, f=0.4139), which corresponds to the experimentally observed peak at 418 nm. The experimentally observed peak at 406 nm for complex **4b** can be assigned to the transition to the twelfth singlet-excited state (S_{12}, f=0.6673, 397.5 nm); the peak at 425 nm for complex **4d** is assigned to S_3 (416.4 nm, f=0.0819). These transition processes all involved admixtures of MLCT and/or LLCT transitions, as well as some ILCT (intra-ligand charge transfer, Table S1 and Figures S2–S5).

3.4 DSSCs performance

The four complexes were used as photosensitizer for DSSCs to estimate their performances. However, complexes **4c** and **4d** show nearly equal performance with complex **4a**. We provide the performance parameters of the iridium complex **4a**- and **4b**-based cells are provided, as well as the performance parameters of the N719-based cell for reference. Figure 4 shows their performance curve. In addition, the photovoltaic performances of these solar cells were measured under AM 1.5 G conditions (100 mW/cm^2), and detailed device parameters are provided in Table 2. The solar cells based on iridium dyes **4a** and **4b** gave similar open-circuiting voltage (V_{oc}) 580 mV, which is comparable to results from early studies that used iridium complexes as photosensitizers [2,16]. Device **4b** showed an overall conversion efficiency of 0.62% and a short-circuit current density of 1.40 mA/cm^2. This is much better than for device **4a**, which gave a 0.19 % and 0.46 mA/cm^2.

To our surprise, the introduction of the dicyanovinyl unit into the *m*-position (relative to aromatic *N*-heterocycle) of the phenyl ring in the ppy or piq ligand induced a significantly enhanced absorption response in a relatively lower energy band. However, the solar cells based on the complexes reported here showed lower cell parameters than those based on similar iridium complexes reported by Ning *et al.* [16]. We suppose that the poor performances should be related to the transition properties of these iridium complexes. The transition contributed to the absorption response of these complexes at longer wavelengths is mainly from the different ppy/piq moieties, according to our TD-DFT calculation (Table S1 and Figures S2–S5). This response contributed little to the current production in the cell, however, due to no contact begtween ppy/piq moieties and the TiO_2 film. This lack of contact may be primarily responsible for the poor cell parameters. It may be that converting one cyano of the dicyanovinyl group in ppy/pic to carboxyl as an anchoring group would improve the electron injection onto TiO_2 film from iridium complexes, and then further enhance the cell parameters.

In order to get more insight into electronic processes in DSSC, electrochemical impedance spectroscopy (EIS) was conducted for devices **4a** and **4b**, which were measured at –0.4 V (Figure 4). A typical EIS spectrum exhibits three semicircles in the Nyquist plot. The electron transport feature in TiO_2 film is generally overlapped with an interfacial recombination in the frequency range from 10^2 to10^3 Hz [17]. Our EIS spectra show only one semicircle, in the middle-frequency range (peak at 10 Hz) in the body-phase plots; in addition, significantly high impedance was observed in Nyquist plots. These results mean that the charge transfer from iridium complexes to TiO_2 films is highly limited,

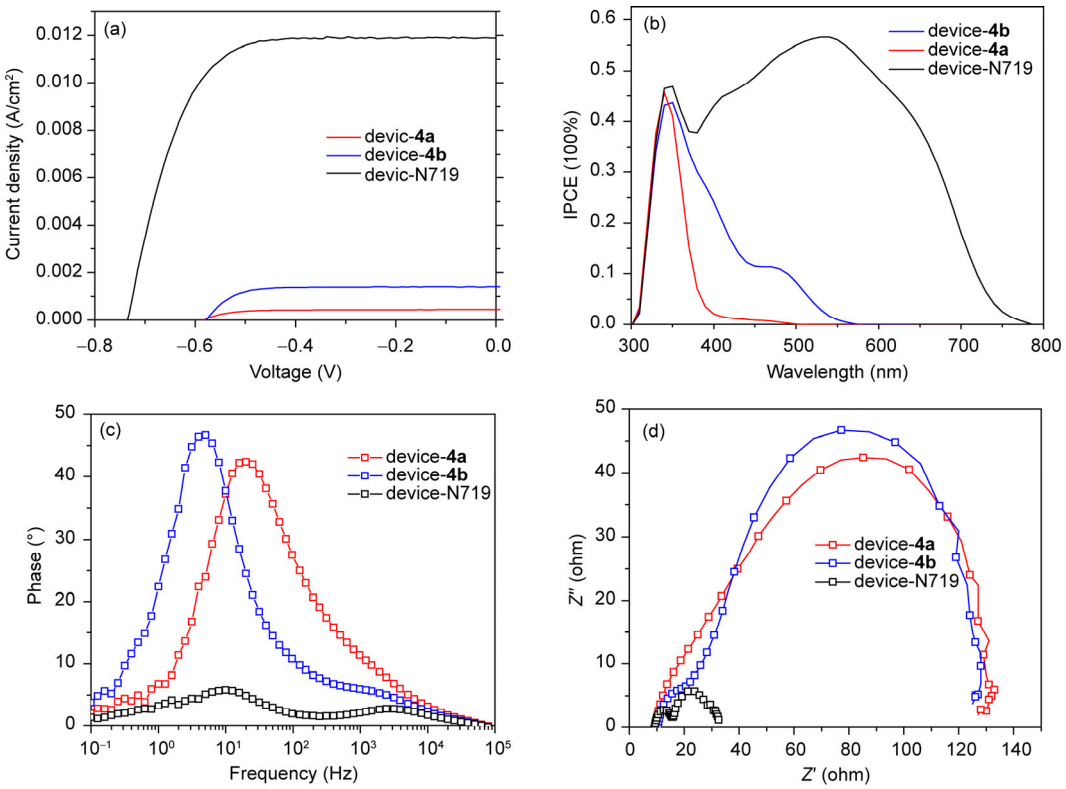

Figure 4 (a) IPCE spectra and (b) photocurrent density-voltage characteristics curve for DSSC devices recorded under illumination of simulated solar light (AG 1.5 G, 100 mW/cm^2). (c) Bode phase plots and (d) Nyquist plots measured in dark at a bias of –0.4 V.

Table 2 Photovoltaic characteristics of DSSCs based on the iridium complexes under 100 mW/cm^2 illumination [a)]

	V_{oc} (V)	J_{sc} (mA/cm^2)	Fill factor (%)	Efficiency (%)
Device-**4a**	0.58	0.46	60.34	0.19
Device-**4b**	0.58	1.40	60.23	0.62
Device-N719	0.73	11.91	62.31	6.05

a) The values in brackets represent the measured maximum value and outside the brackets is a mean value.

resulting in poor performance parameters for these iridium complex-based cells.

4 Conclusions

We synthesized and characterized a new series of iridium complexes with dicyanovinyl-grafted phenylpyridine and 1-phenylisoquinoline as ligands, and with pyridine-2,4-dicarboxyl acid or 2,2′-bipyridine-4,4′-dicarboxyl acid as ancillary anchoring ligands. These iridium complexes showed considerable absorption response in the visible light range from 400 to 525 nm. Our TD-DFT calculations suggest that the electron transition in the low-energy region for complexes **4a–4d** is mainly attributed to MLCT and/or LLCT transition. Furthermore, a noteworthy red-shifted (60–80 nm) PL emission of iridium complexes **4a** and **4b** in dye-doped PMMA film was observed, compared with their DMSO solution. The **4b**-based device showed the best performance parameters. Even so, all of the iridium-complex-based devices showed unanticipated performance parameters due to the limitation of electron-transfer from dyes to TiO_2 film.

Supporting information

The supporting information is available online at chem.scichina.com and link.springer.com/journal/11426. The supporting materials are published as submitted, without typesetting or editing. The responsibility for scientific accuracy and content remains entirely with the authors.

This work was supported by the Fundamental Research Funds for the Central Universities (08143034), the National Basic Research Program of China (2013CB328705, 2013CB328706), and the National Natural Science Foundation of China (61275034, 61106123).

1 (a) Lamansky S, Djurovich P, Murphy D, Abdel-Razzaq F, Lee HE, Adachi C, Buttows PE, Forrest SR, Thompson ME. Highly phosphorescent bis-cyclometalated iridium complexes: synthesis, photophys-

ical characterization, and use in organic light emitting diodes. *J Am Chem Soc*, 2001, 123: 4304–4312; (b) Nazeeruddin MK, Humphry-Baker R, Berner D, Rivier S, Zuppiroli L, Graetzel M. Highly phosphorescence iridium complexes and their application in organic light-emitting devices. *J Am Chem Soc*, 2003, 125: 8790–8797; (c) Kim J, Shin IS, Kim H, Lee JK. Efficient electrogenerated chemiluminescence from cyclometalated iridium(III) complexes. *J Am Chem Soc*, 2005, 127: 1614–1615; (d) Lee SJ, Park KM, Yang KY, Kang YJ. Blue phosphorescent Ir(III) complex with high color purity: *fac*-tris(2′,6′-difluoro-2,3′-bipyridinato-*N*,$C^{4'}$)iridium(III). *Irorg Chem*, 2009, 48: 1030–1037; (e) Chiu YC, Hung JY, Chi Y, Chen CC, Chang CH, Wu CC, Cheng YM, Yu YC, Lee GH, Chou PT. En route to high external quantum efficiency (~12%), organic true-blue-light-emitting diodes employing novel design of iridium(III) phosphors. *Adv Mater*, 2009, 21: 2221–2225; (f) Seo HJ, Yoo KM, Song MK, Park JS, Jin SH, Kim YI, Kim JJ. Deep-blue phosphorescent iridium complexes with picolinic acid N-oxide as the ancillary ligand for high efficiency organic light-emitting diodes. *Org Electron*, 2010, 11: 564–572

2 Yuan YY, Zhang JY, Yu ZT, Feng JY, Lou WJ, Ye JH, Zou ZG. Impact of ligand modification on hydrogen photogeneration and light-harvesting applications using cyclometalated iridium complexes. *Inorg Chem*, 2012, 51: 4123–4133

3 (a) Lo KKW, Hui WK, Chung CK, Tsang KHK, Lee TKM, Li CK, Lau JSY, Ng DCM. Luminescent transition metal complex biotin conjugates. *Coord Chem Rev*, 2006, 250: 1724–1736; (b) Lo KKW, Chung CK, Lee TKM, Lui LK, Tsang KHK, Zhu N. New Luminescent cyclometalated iridium(III) diimine complexes as biological labeling reagents. *Inorg Chem*, 2003, 42: 6886–6897; (c) Lo KKW, Ng DCM, Chung CK. First examples of luminescent cyclometalated iridium(III) complexes as labeling reagents for biological substrates. *Organometallics*, 2001, 20: 4999–5001; (d) Chen H, Zhao Q, Wu Y, Li F, Yang H, Yi T, Huang C. Selective phosphorescence chemosensor for homocysteine based on an iridium(III) complex. *Inorg Chem*, 2007, 46: 11075–11081

4 (a) Tam AYY, Tsang DPK, Chan MY, Zhu NY, Yam VWW. A luminescent cyclometalated platinum(II) complex and its green organic light emitting device with high device performance. *Chem Commun*, 2011, 47: 3383–3385; (b) Buda M, Kalyuzhny G, Bard AJ. Thin-film solid-state electroluminescent devices based on tris(2,2'-bipyridine) ruthenium(II) complexes. *J Am Chem Soc*, 2002, 124: 6090–6098; (c) Cheng YM, Yeh YS, Ho ML, Chou PT. Dual room-temperature fluorescent and phosphorescent emission in 8-quinolinolate osmium(II) carbonyl complexes: rationalization and generalization of intersystem crossing dynamics. *Inorg Chem*, 2005, 44: 4594–4603; (d) Lee SJ, Park JS, Song MK, Shin IA, Kim YI, Lee JW, Kang JW, Gal YS, Kang SW, Lee JY, Jung SH, Kim HS, Chae MY, Jin SH. Synthesis and characterization of red-emitting iridium(III) complexes for solution- processable phosphorescent organic light-emitting diodes. *Adv Funct Mater*, 2009, 19: 2205–2212

5 (a) Baranoff E, Yum JH, Graetzel M, Nazeeruddin MK. Cyclometallated iridium complexes for conversion of light into electricity and electricity into light. *J Organometal Chem*, 2009, 694: 2661–2670; (b) Shinpuku Y, Inui F, Nakai M, Nakabayashi Y. Synthesis and characterization of novel cyclometalated iridium(III) complexes for nanocrystalline TiO_2-based dye-sensitized solar cells. *J Photochem Photobio A: Chem*, 2011, 222: 203–209

6 Mayo EI, Kilsa K, Tirrell T, Djurovich PI, Tamayo A, Thompson ME, Lewis NS, Gray HB. Cyclometalated iridium(III)-sensitized titanium dioxide solar cells. *Photoch Photobio Sci*, 2006, 5: 871–873

7 Schwartz KR, Chitta RH, Bohnsack JN, Ceckanowicz DJ, Miró P, Cramer CJ, Mann KR. Effect of axially projected oligothiophene pendants and nitro-functionalized diimine ligands on the lowest excited state in cationic Ir(III) bis-cyclometalates. *Inorg Chem*, 2012, 51: 5082–5094

8 Yan QF, Fan YP, Zhao DH. Unusual temperature-dependent photophysics of oligofluorene-substituted tris-cyclometalated iridium complexes. *Macromolecules*, 2012, 45: 133–141

9 Sun JF, Wu WH, Guo HM, Zhao JZ. Visible-light harvesting with cyclometalated iridium(III) complexes having long-lived ^{3}IL excited states and their application in triplet-triplet-annihilation based up-conversion. *Eur J Inorg Chem*, 2011: 3165–3173

10 (a) Hallett AJ, Ward BD, Kariuki BM, Pope SJA. Neutral and cationic cyclometallated Ir(III) complexes of anthra[1,2-*d*]imidazole-6, 11-dione-derived ligands: syntheses, structures and spectroscopic characterisation. *J Organometallic Chem*, 2010, 695: 2401–2409; (b) Hallett AJ, White N, Wu WH, Cui XN, Horton PN, Coles SJ, Zhao JZ, Pope SJA. Enhanced photooxidation sensitizers: the first examples of cyclometalated pyrene complexes of iridium(III). *Chem Commun*, 2012, 48: 10838–10840

11 Wang DD, Wu Y, Jiao B, Dong H, Zhou GJ, Wang G, Wu ZX. Wide tuning of emission color of iridium(III) complexes from green to deep red via dicyanovinyl substituent effect on 2-phenylpyridine ligands. *Org Electron*, 2013, 14: 2233–2242

12 Ito S, Murakami TN, Comte P, Liska P, Grätzel C, Nazeeruddin MK, Grätzel M. Fabrication of thin film dye sensitized solar cells with solar to electric power conversion efficiency over 10%. *Thin Solid Films*, 2008, 516: 4613–4619

13 Neve F, La Deda M, Crispini A, Bellusci A, Puntoriero F, Campagna S. cationic cyclometalated iridium luminophores: photophysical, redox, and structural characterization. *Organometallics*, 2004, 23: 5856–5863

14 Tamayo AB, Garon S, Sajoto T, Djurovich PI, Tsyba IM, Bau R, Thompson ME. Cationic bis-cyclometalated iridium(III) diimine complexes and their use in efficient blue, green, and red electroluminescent devices. *Inorg Chem*, 2005, 44: 8723–8732

15 Wang ZS, Kawauchi H, Kashima T, Arakawa H. Significant influence of TiO_2 photoelectrode morphology on the energy conversion efficiency of N719 dye-sensitized solar cell. *Coord Chem Rev*, 2004, 248: 1381–1389

16 Ning Z, Zhang Q, Wu W, Tian H. Novel iridium complex with carboxyl pyridyl ligand for dye-sensitized solar cells: high fluorescence intensity, high electron injection efficiency? *J Organomet Chem*, 2009, 694: 2705–2711

17 Kuang DB, Ito S, Wenger B, Klein C, Moser JE, Humphry-Baker R, Zakeeruddin SM, Gratzel M. High molar extinction coefficient heteroleptic ruthenium complexes for thin film dye-sensitized solar cells. *J Am Chem Soc*, 2006, 128: 4146–4154